

# Modeling and forecast of polar motion excitation functions for short-term polar motion prediction

T.M. Chin, R.S. Gross, J.O. Dickey

Jet Propulsion Laboratory  
California Institute of Technology

The research described in this poster was carried out at the Jet Propulsion Laboratory, California Institute of Technology, under a contract with the National Aeronautics and Space Administration (NASA).

# Motivation

The dynamics of polar motion (in the range of daily to sub-decadal frequencies) is dominated by the Chandler wobble, a resonant oscillator excited by variations of atmospheric, oceanic, and ground water origins. Understanding the origin of the excitation of the polar motion including the Chandler wobble remains incomplete. A simple stochastic model of the excitation function, such as a random walk, is generally sufficient for operational earth orientation analyses due to availability of various measurements for updates. More accurate models are still desirable for short-term prediction, especially during the observation voids between measurement epochs. Moreover, spacecraft navigation typically requires estimates of the earth orientation parameters up to 7 days of lead time.

The goal of this study is in improvement of the short-term prediction of the polar motion in the context of state-space modeling suitable for the Kalman filter operations, such as the Kalman Earth Orientation Filter (KEOF) at Jet Propulsion Laboratory. Empirical periodicities are determined from an analyzed polar motion excitation function time series, and these periodicities are to be extrapolated in time. Fourier series expansion is a standard technique for spectral analysis; however, the sinusoidal Fourier basis functions lack the time-local specificity that is characteristics of the polar motion

time series. In particular, the magnitude, frequency, and phase need to be allowed to vary slowly in time for an effective sinusoidal representation for polar motion. While a variety of techniques are reported in the literature for direct prediction of polar motion time series, this report focuses on modeling and prediction of the excitation function.

# Summary

Short-term forecast of the polar motion is considered by introducing a prediction model for the excitation function which drives the polar motion dynamics. The excitation function model consists of a slowly varying trend, periodic modes with annual and several sub-annual frequencies (down to the 13.6-day fortnightly tidal period), and a transient decay function with a time constant of 1.5 days. Each periodic mode is stochastically specified using an order-two autoregression process, allowing its frequency, phase, and amplitude to vary in time within a statistical tolerance. The model is used to time-extrapolate the excitation function series, which is then used to generate a polar motion forecast dynamically. Skills of this forecast method is evaluated by comparison to the C-04 polar motion series in hindcast experiments. Over the lead-time horizon of four months, the proposed method has performed equally well to some of the state-of-art polar motion prediction methods, none of which features forecasting of the excitation function. The annual mode in the  $\chi_2$  component is energetically the most dominant periodicity. The modes with longer periods, annual and semi-annual in particular, are found to contribute more significantly to forecast accuracy than those with shorter periods.

# Models

## 1. Polar motion (KEOF)

The polar motion  $\mathbf{p}$  is represented by a fixed-period oscillator whose amplitude and phase are modulated by the excitation function  $\boldsymbol{\chi}$  as

$$\mathbf{p} + \frac{i}{\sigma_{cw}} \dot{\mathbf{p}} = \boldsymbol{\chi} \quad (1)$$

where  $i \equiv \sqrt{-1}$ ,  $\dot{\mathbf{p}} \equiv d\mathbf{p}/dt$ ,  $\sigma_{cw} \equiv \sigma(1 + i/2Q)$  is the complex-valued (damped) frequency of the Chandler wobble,  $\mathbf{p} \equiv P_x(t) - iP_y(t)$  where  $P_x(t)$  and  $P_y(t)$  are the  $x$ - and  $y$ -components of polar motion, and  $\boldsymbol{\chi} \equiv \chi_1(t) + i\chi_2(t)$  where  $\chi_1(t)$  and  $\chi_2(t)$  are the  $x$ - and  $y$ -components, respectively, of the excitation function. The Chandler frequency parameters used here are  $\sigma = 2\pi/433$  cycles per day and  $Q = 170$  corresponding to a decay time of 64 years.

## 2. Excitation function analysis (KEOF)

$$\chi_1(t) = \mu_1(t) \quad (2)$$

$$\chi_2(t) = S(t) + \mu_2(t) \quad (3)$$

where  $\mu_1(t)$  and  $\mu_2(t)$  are random walk processes

$$\dot{\mu}_j(t) = w_j^\mu(t), \quad j = 1, 2 \quad (4)$$

and  $S(t)$  is a stochastic oscillator given by

$$\ddot{S} + \alpha\dot{S} + \beta S = w^s(t) \quad (5)$$

Above model is fine for analysis (data update); however, it leads to a not-so-good prediction model:

$$\chi_1(t|t_0) = \mu_1(t_0) \quad (6)$$

$$\chi_2(t|t_0) = \mu_2(t_0) + S(t|t_0) \quad (7)$$

where  $(t|t_0)$  denotes “forecast for  $t \geq t_0$  based on the data-updated analysis up to time  $t_0$ ”. This forecast can be problematic because it persists some instantaneous values of the random-walk processes.

### 3. Excitation function prediction

A more general model for the excitation function is

$$\chi_j(t) = \bar{\chi}_j(t) + \sum_{k=1}^{K_j} S_{jk}(t), \quad j = 1, 2 \quad (8)$$

$$\ddot{S}_{jk} + \alpha_{jk}\dot{S}_{jk} + \beta_{jk}S_{jk} = w_{jk}^s(t) \quad (9)$$

where  $\bar{\chi}_j$  is the trend,  $w_{jk}^s(t)$  are mutually independent white noise processes, and  $\alpha_{jk}$  and  $\beta_{jk}$  are given constants. The frequency and other parameters for the periodic (and non-periodic) modes  $S_{jk}$  is given in Table 1.

# Results

- Hindcasting experiments have been conducted over a five-year duration from 1 October 1995 to 30 September 2000. The C-04 daily polar motion time series analysis produced by the International Earth Rotation Service is used as the ground truth in the experiments. Forecasts of up to a 365-day lead-time are produced during the experimental period at a one-week interval, resulting in 261 samples for each experiment. The root-mean-squares (RMS) error between the forecast time series and the C-04 analysis series is used primarily as the measure of accuracy.
- Figure 6 demonstrates that the periodic mode model for the excitation function leads to significantly more accurate forecasts of polar motion than the model designed for operational analysis in KEOF. The RMS value of 2 mas at 5-day represents nearly 20% reduction in forecast error. At 20-day, the error becomes less than half.
- Figure 7 demonstrates that a polar motion forecast method that relies dynamically on a prediction of the excitation function (using the proposed periodic mode model in particular) can be just as accurate as methods that are non-dynamic (i.e., functional approximation or statistical extrapolation applied *directly* on the

polar motion time series), especially for the short-term (less than four months) forecast of our interest. Note that each error curves have been computed under different experimental conditions including the choice of time-windows; thus, comparison can be made only approximately. See Figure 6 for some estimates of the significant level.

- Figure 8 demonstrates that the modes with longest periods (annual and semi-annual) and the smooth tapering mode (Langevin process with time constant of 1.5 days) are the most important components of the proposed excitation function model in terms of accuracy of polar motion forecast. The tapering (dotted line) displays its effectiveness only for the first 2-3 days. The positive effects of the annual and semi-annual modes are evident even at extremely short lead-times (by comparison of dash-dot and dotted lines). The shorter periodic modes, including the fortnightly periodicity, had small contributions to accuracy of the forecast.
- The prediction error is consistently lower for  $\chi_1$  than  $\chi_2$ . One reason for this is the asymmetry in the distribution of the continents and oceans on the global surface, so that the oceans can contribute more on variations in  $\chi_1$  than  $\chi_2$ . Note that  $\chi_1$  affects the accuracy of  $P_y$  more than  $P_x$ , while  $\chi_2$  affects  $P_x$  more.

$\chi_1$	$\chi_2$	period	damping	variance	notes
yes	yes	0	1.5	200	tapering process
yes	yes	365.26	0	$2 \times 10^{-6}$	annual mode
yes	yes	182.62	0	$2 \times 10^{-6}$	semi-annual mode
yes	no	121.75	0	$2 \times 10^{-6}$	ter-annual mode
no	yes	60.88	0	$2 \times 10^{-8}$	
yes	no	45.66	0	$2 \times 10^{-8}$	
yes	no	36.53	0	$2 \times 10^{-8}$	
yes	no	22.04	0	$2 \times 10^{-8}$	
yes	yes	13.66	0	$2 \times 10^{-8}$	fortnightly tidal period

**Table 1**

Parameters of the periodic and tapering modes. Whether or not the particular mode is used for the given  $\chi$  component is indicated by “yes” or “no”. The units are “days” for the period and damping time-constant and “(mas)<sup>2</sup> per day” for the variance of the driving process.

# Figures

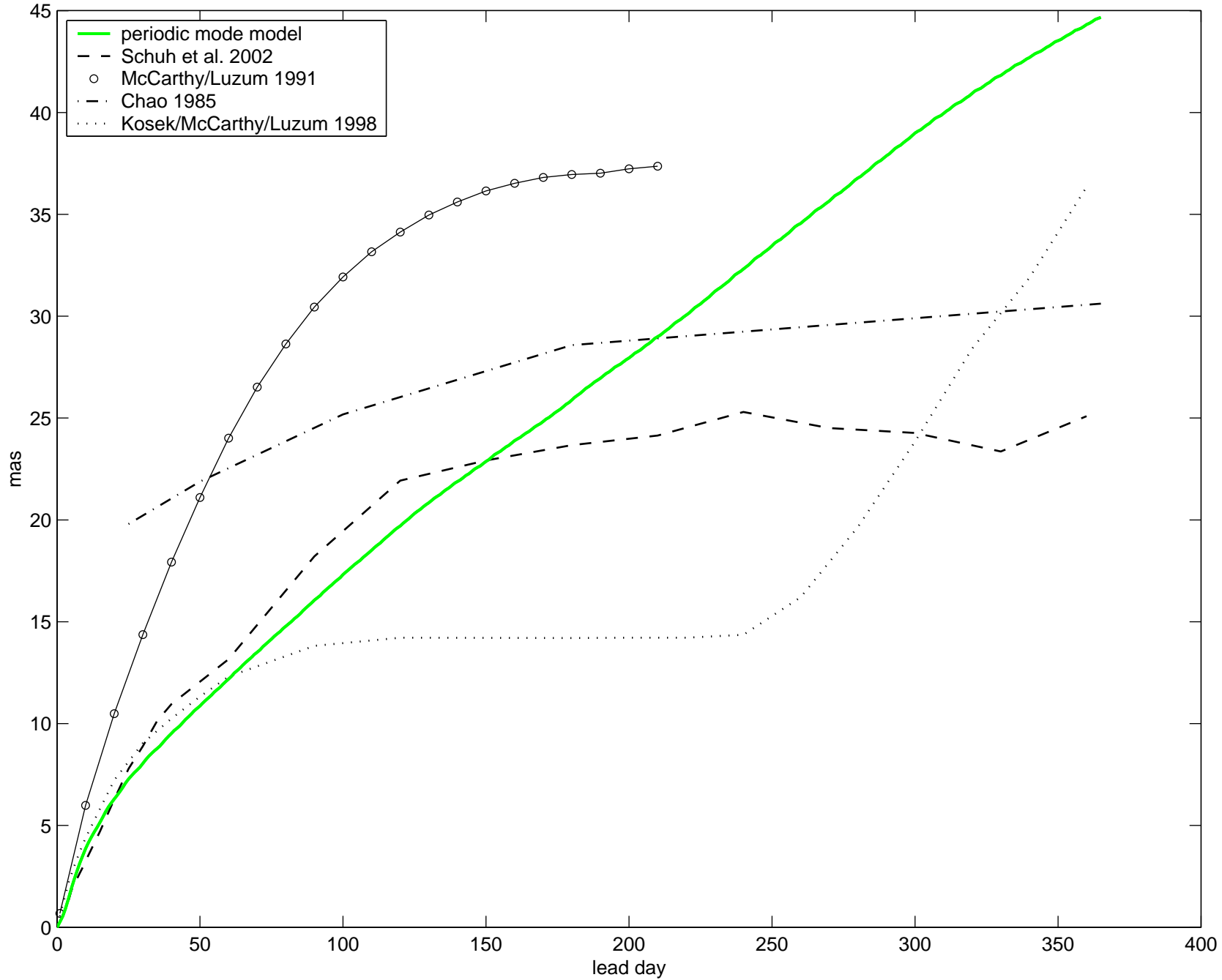
1. Time series of the  $\chi_1$  component of the excitation function produced by KEOF (top panel, dashed line) and some of its additive subcomponents: the 13.6-day period mode (second panel), the annual and semi-annual modes (third panel, solid and dashed lines respectively), and the Langevin process (bottom panel). The units are “day” for the horizontal and “mas” for the vertical axes. The dotted line on the top panel is the sum of all subcomponents, demonstrating that the sum and the data (dashed line) are nearly equal.
2. The same as Fig. 1, except that the  $\chi_2$  component and its subcomponents are plotted.
3. Power spectral densities of  $\chi_1$  (top) and  $\chi_2$  (bottom) produced by KEOF. The labeled peaks are used to identify the frequencies of the periodic modes. The numbered labels are associated with those harmonic to the annual period where the numbers represent the order of the harmonics. The label “F” denotes the fortnightly tidal period, while the label “M” points to a monthly period.
4. The same as Fig. 1, except that the predicted time series are shown.

5. The same as Fig. 2, except that the predicted time series are shown.
6. RMS errors for the polar motion forecasts using the operational analysis model (dashed line) and the periodic mode model (solid line) of excitation function, with 95% confidence levels based on the chi-squared probability distribution.
7. RMS errors for the polar motion forecasts, up to a lead-time of one year, using the periodic mode model for the excitation function (solid line) and three other published forecast methods that do not involve forecasting of excitation function (broken lines). Note that the error curves have been computed under different experimental conditions, so that a quantitative comparison of the errors is not possible.
8. RMS errors for the polar motion forecasts using the full set of periodic modes (solid thin line); only the tapering mode (dotted line); using the fortnightly, semi-annual, and annual modes (dashed line); and using the tapering, semi-annual, and annual modes (dash-dot line).

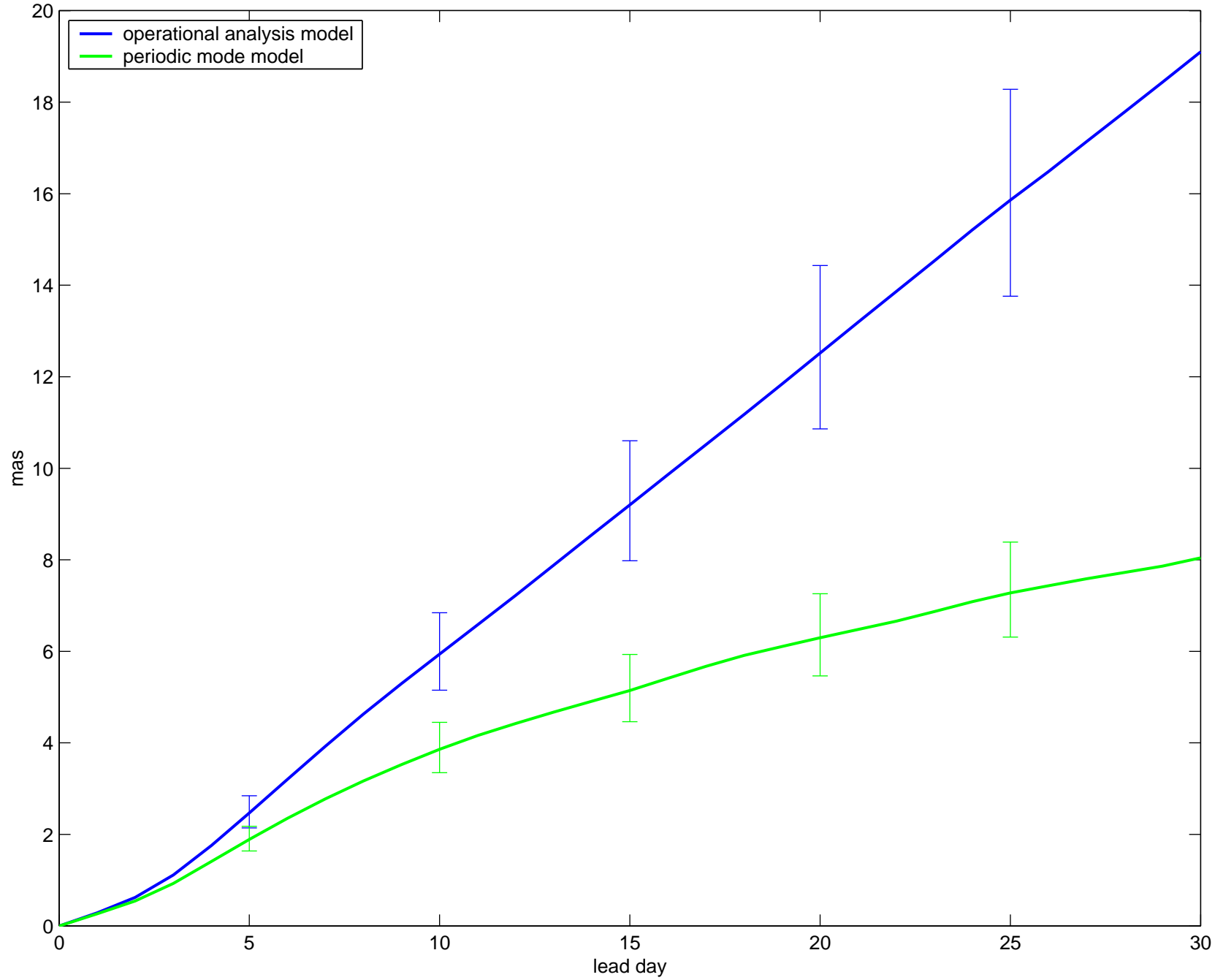
# Notes

- One of the modes in (9) is a special, non-periodic function used as a *tapering function* that makes smooth transition from the most recent filtered value to the steady state (periodic) behavior. This is given by setting  $\beta_{jk} = 0$ , so that  $d(\dot{S}_{jk} + \alpha_{jk}S_{jk})/dt = w_{jk}^s$ . The tapering function  $S_{jk}$  is then a *Langevin process* driven by a random walk (which is in turn driven by the white noise  $w_{j0}^s$ ).
- The unit “mas” is milliarcsecond, which translates to about 3 *cm* of distance on the surface of Earth.
- As a possible improvement to the method described here, the set of periodicities to model can be chosen more objectively by application of *singular spectrum analysis* (Keppenne and Ghil, 1992). Statistically dominant periodicities can be selected based on eigen-decomposition of an empirical covariance matrix assuming stationarity. This approach is under investigation.

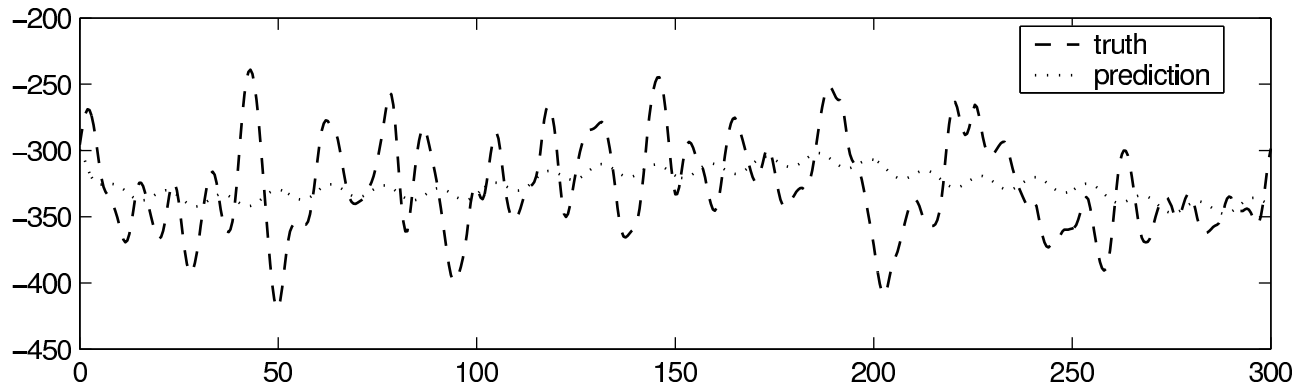
PM prediction error (1995/10/1 – 2000/9/24)



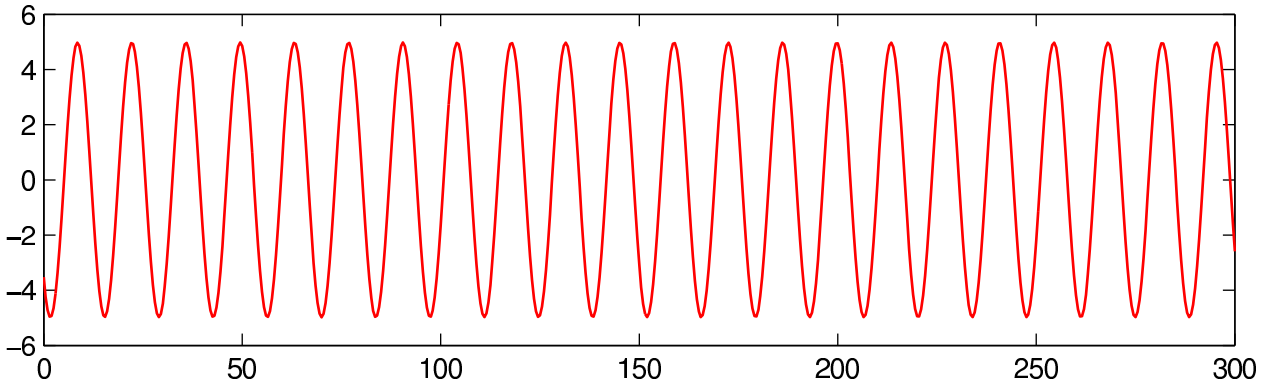
PM prediction error (1995/10/1 – 2000/9/24)



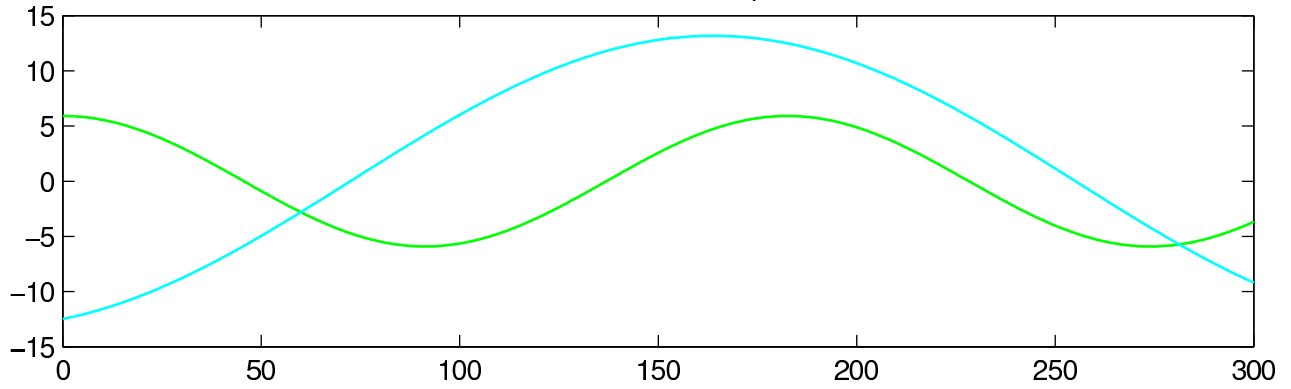
Prediction of  $\chi_2$  (starting on 1996/1/1)



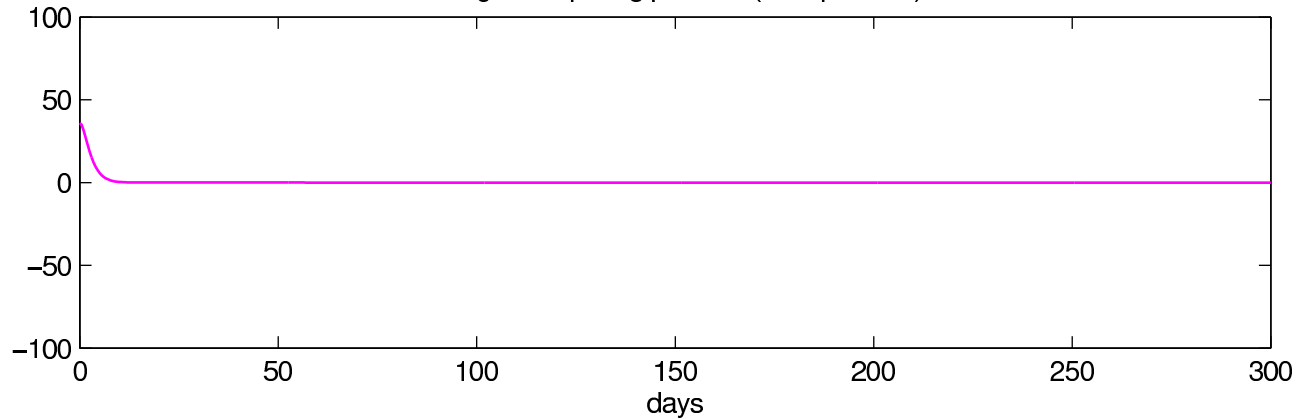
fortnightly tidal period (13.6 days)



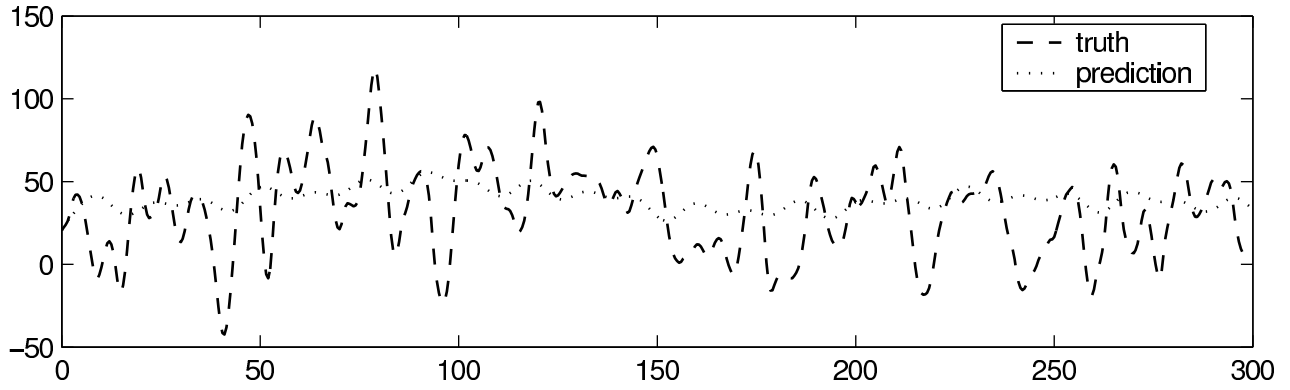
annual & semi-annual periods



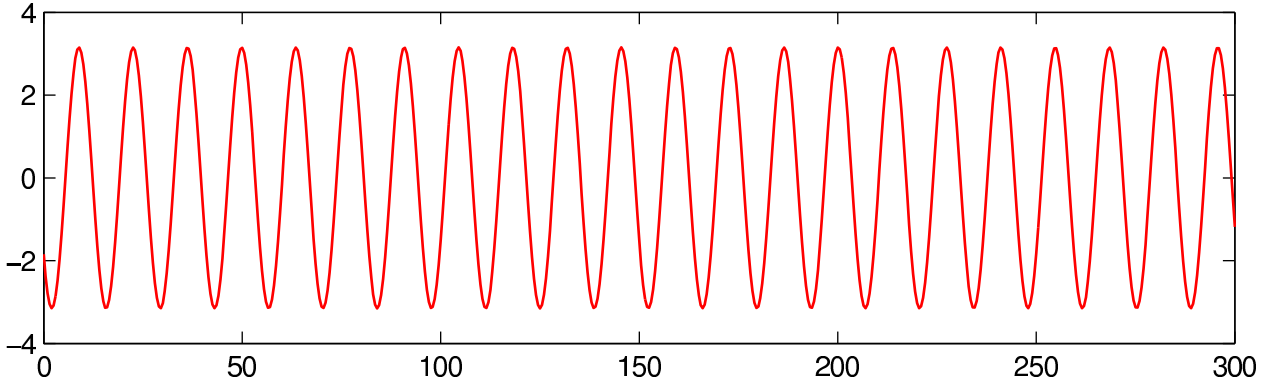
Langevin tapering process (non-periodic)



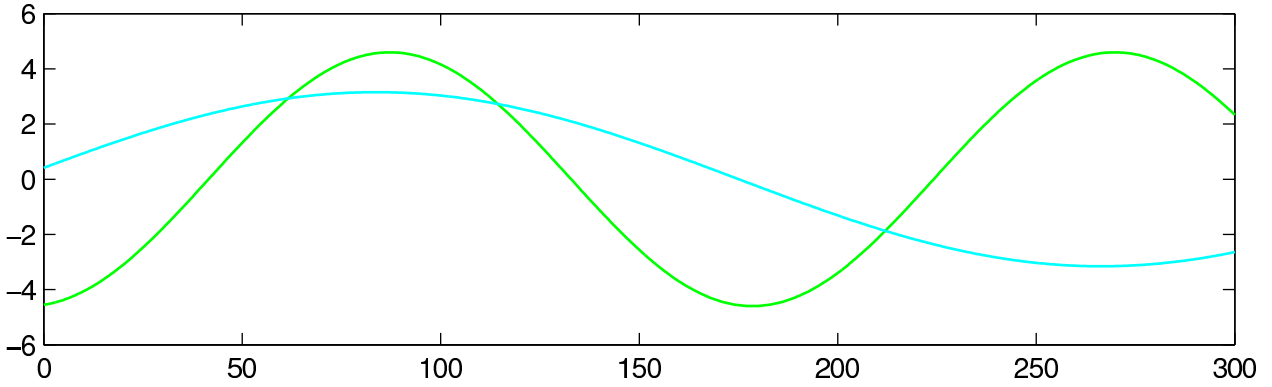
Prediction of  $\chi_1$  (starting on 1996/1/1)



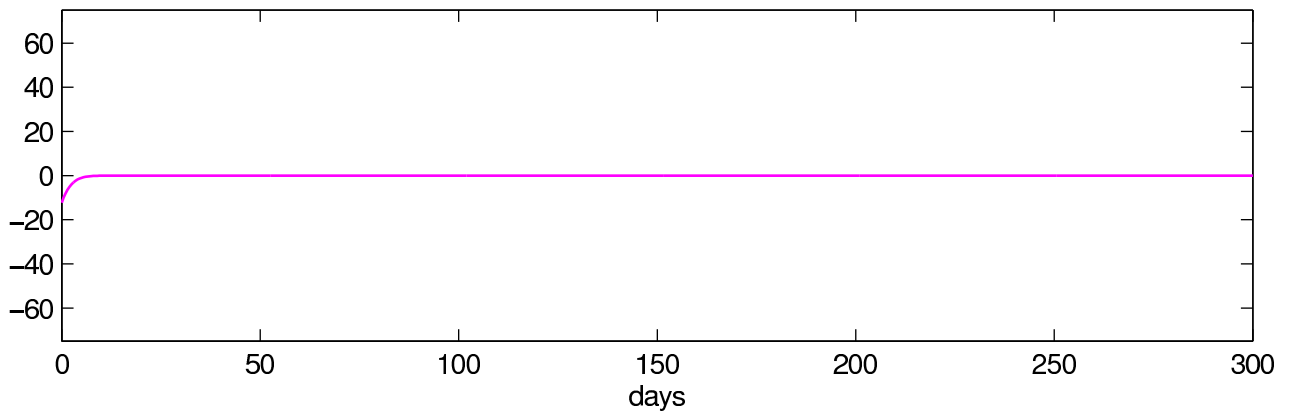
fortnightly tidal period (13.6 days)

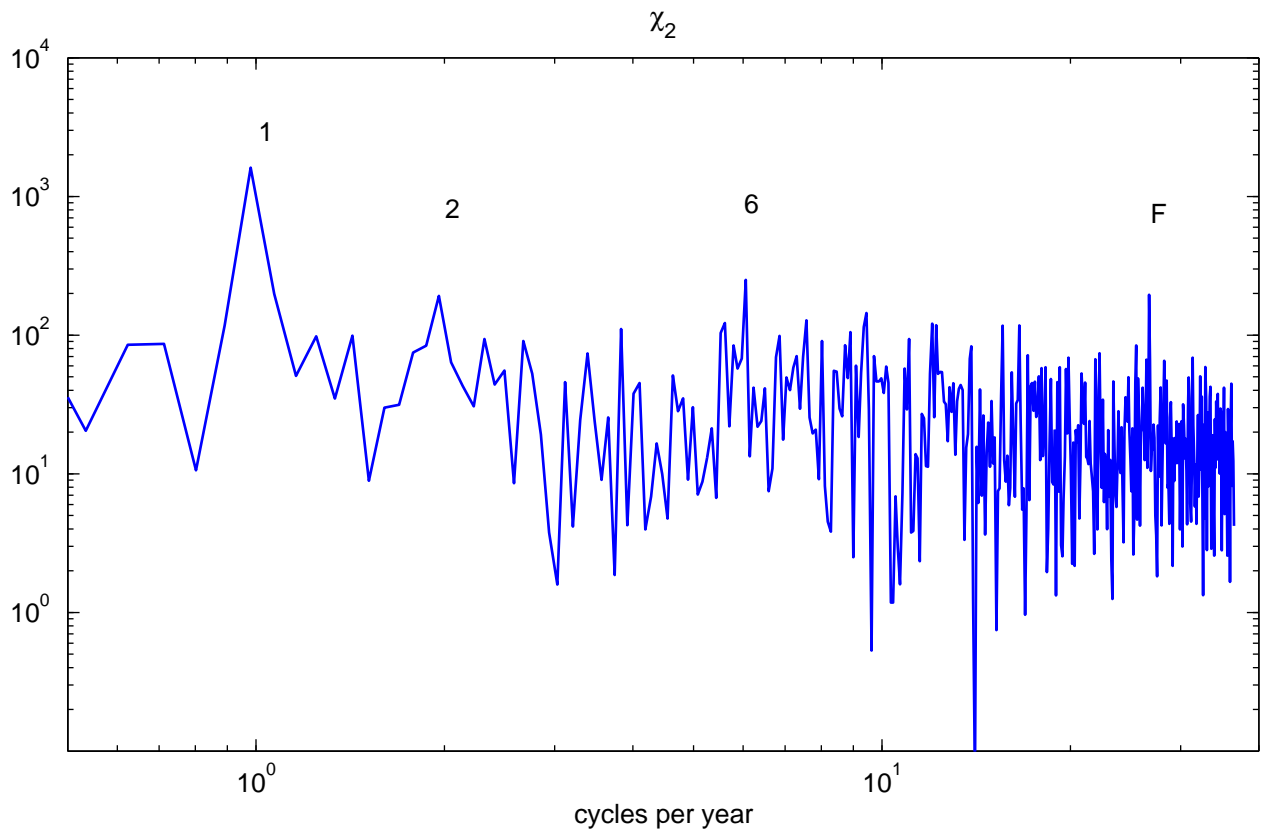
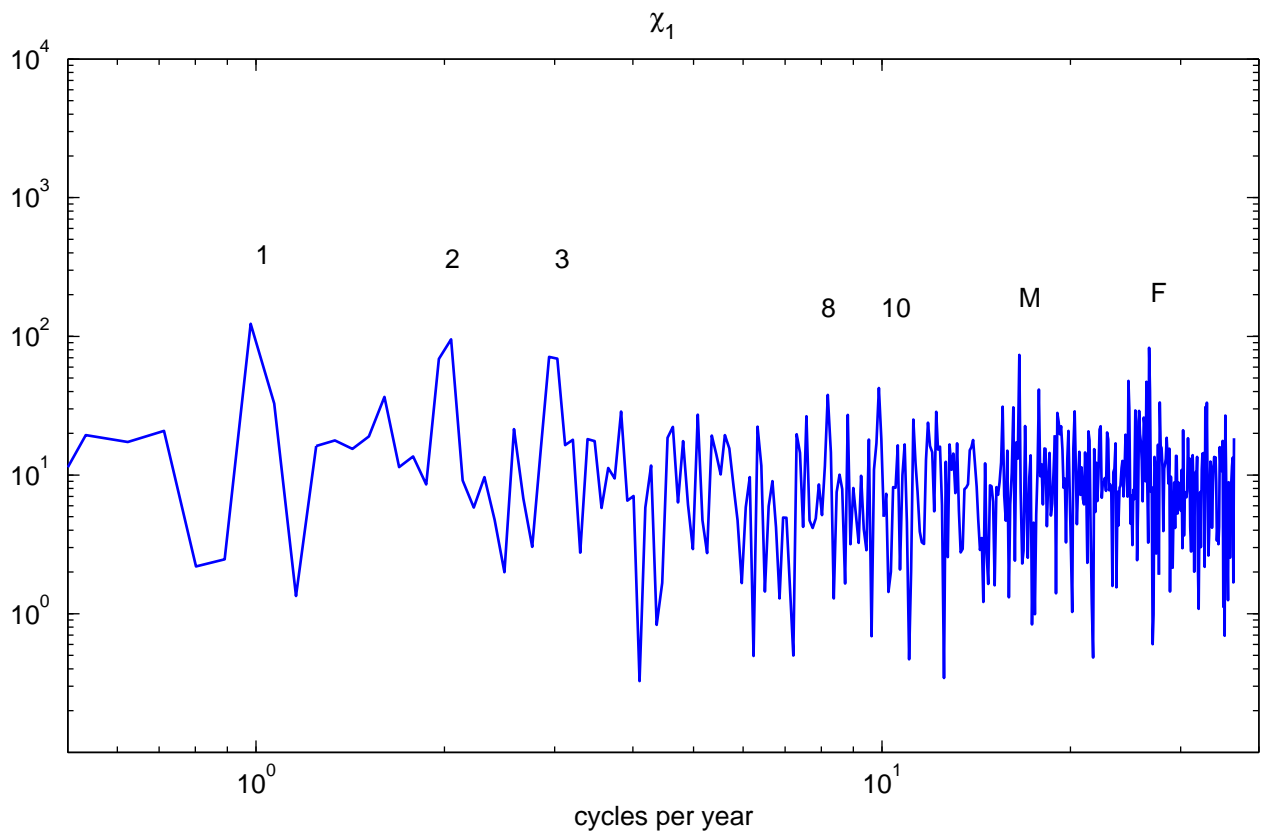


annual & semi-annual periods

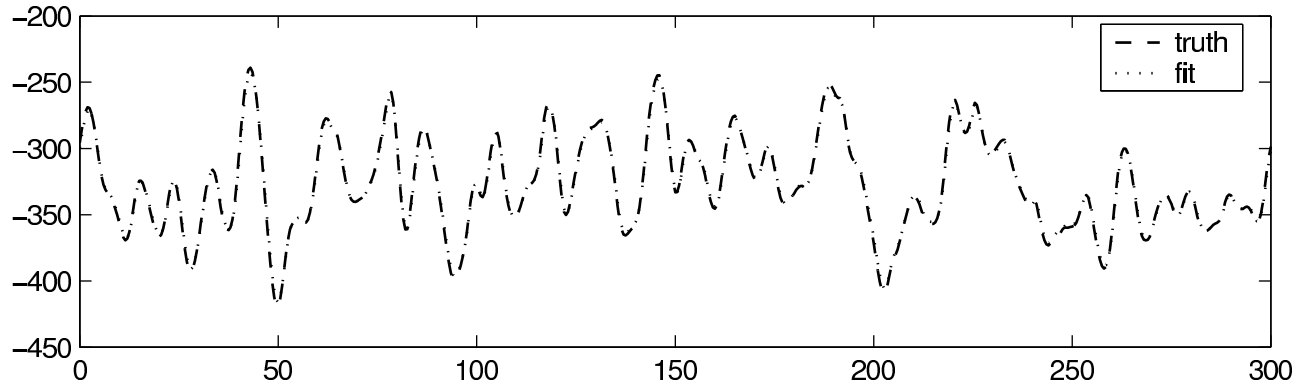


Langevin tapering process (non-periodic)

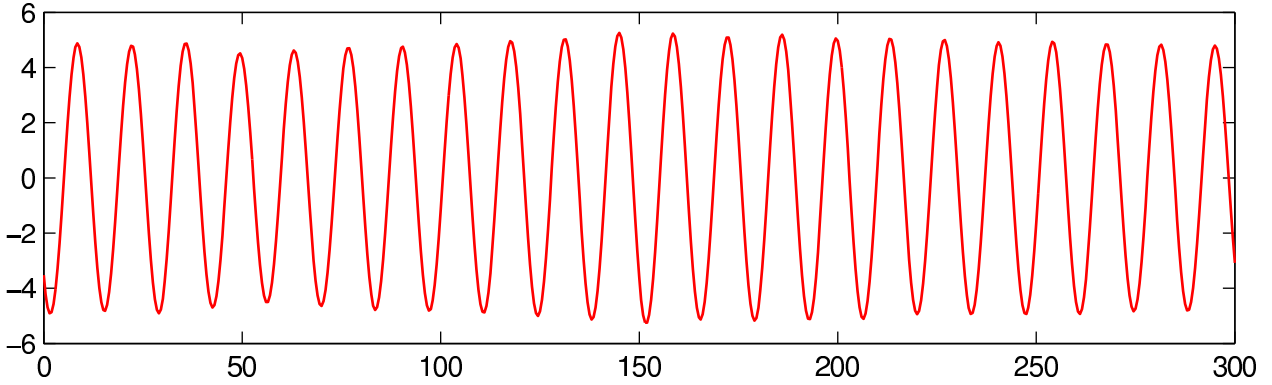




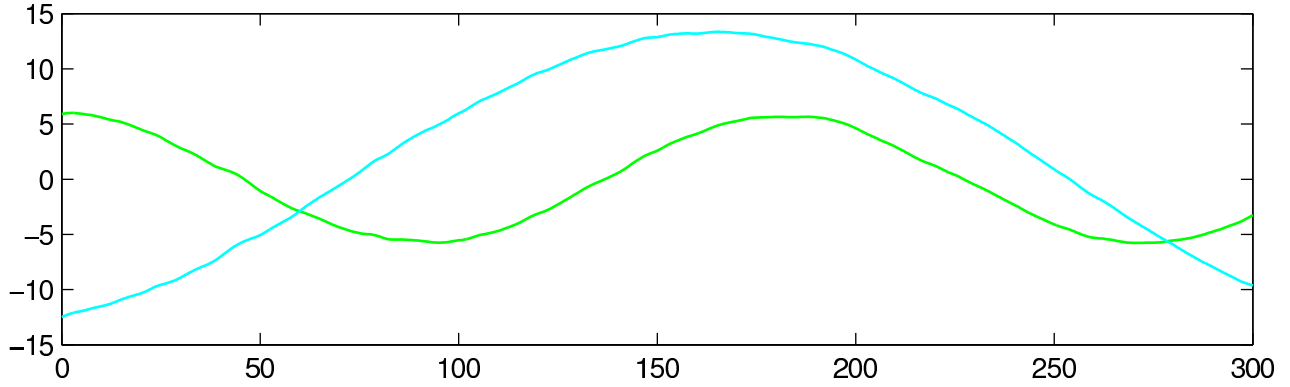
Expansion of  $\chi_2$  (starting on 1996/1/1)



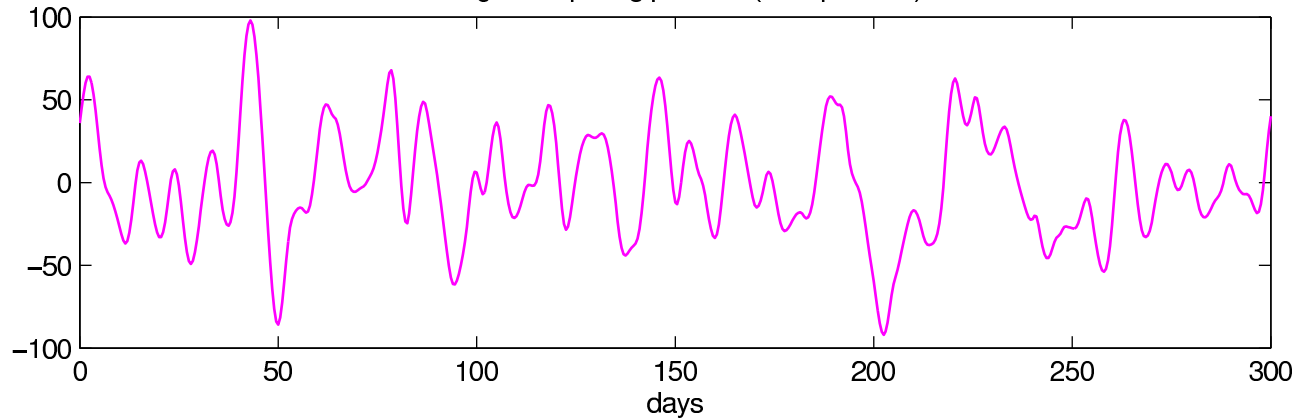
fortnightly tidal period (13.6 days)



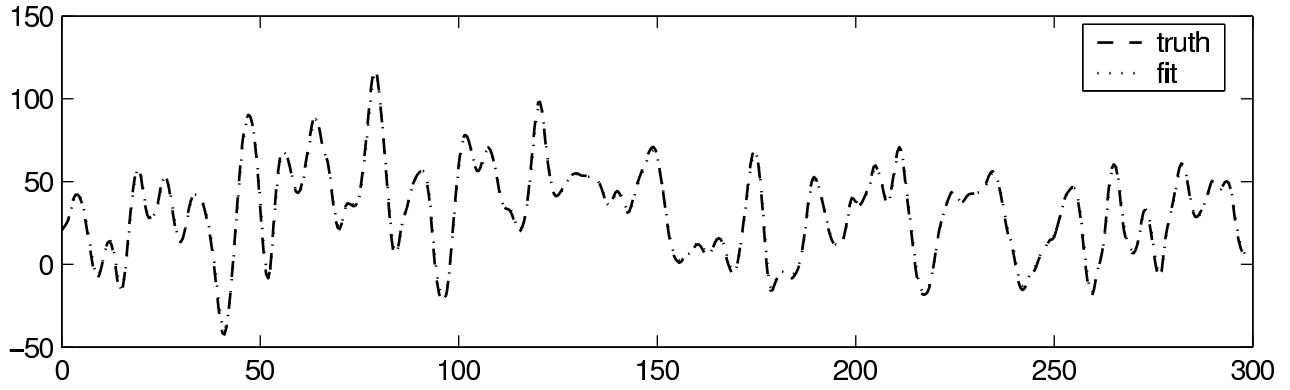
annual & semi-annual periods



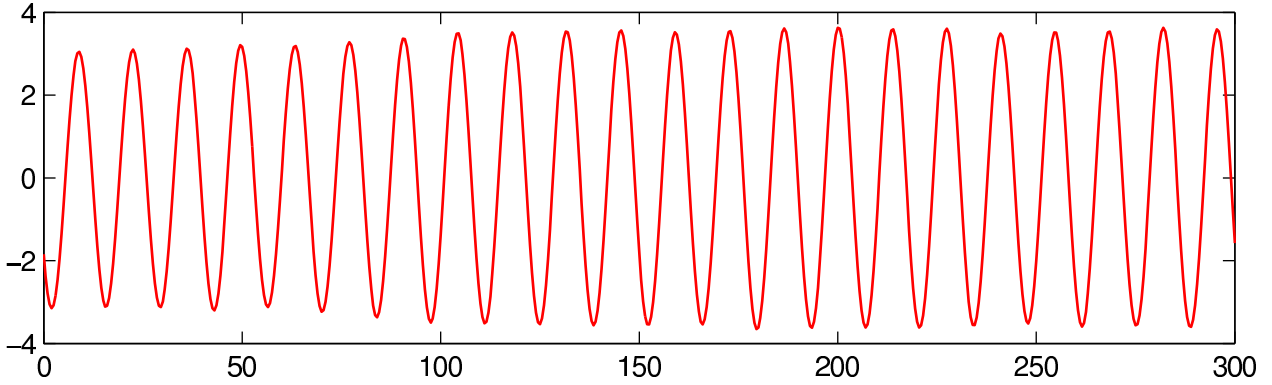
Langevin tapering process (non-periodic)



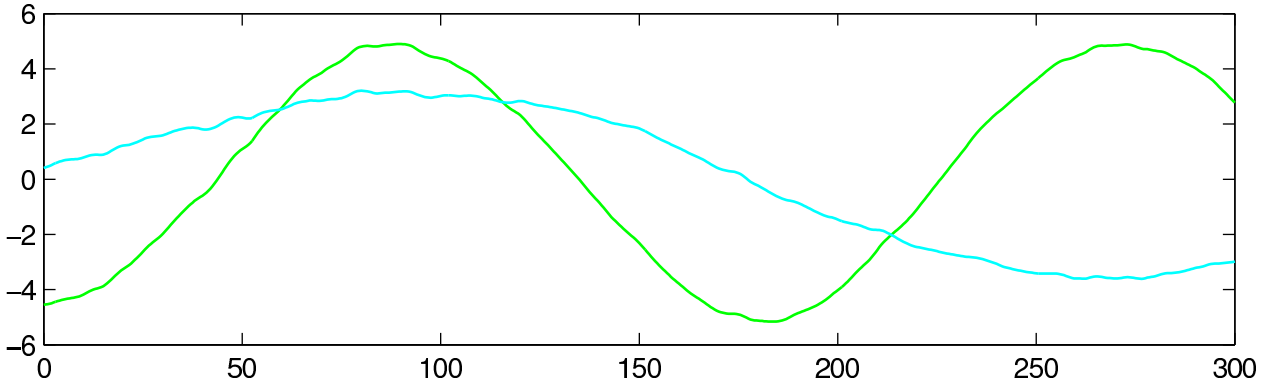
Expansion of  $\chi_1$  (starting on 1996/1/1)



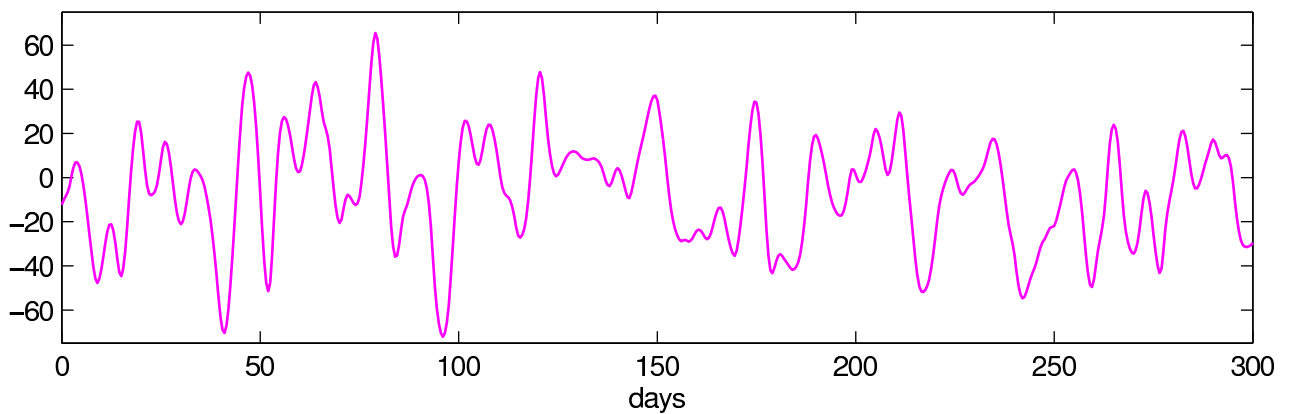
fortnightly tidal period (13.6 days)



annual & semi-annual periods



Langevin tapering process (non-periodic)



PM prediction error (1995/10/1 – 2000/9/24)

